

## Inhomogeneities and dumping of high frequency electromagnetic field in the space close to porous wall

**Abstract.** The aim of this paper is an analysis of distribution of a high frequency electromagnetic field ( $f=2.4$  GHz) behind the heterogeneous wall. The analysis is connected with some typical structures of the wall made of either: a solid brick or two types of hollow clay bricks. The influence of internal geometry and the relative homogeneous properties of the components on field distribution are presented and discussed. The relation between electric conductivity of the clay and structures of air holes are examined too. The presented results give some information about field distribution around materials which consist of some non-ideal, absorbing dielectrics.

**Streszczenie.** Celem publikacji jest analiza rozkładu pola elektromagnetycznego wielkiej częstotliwości w obszarze zawierającym ścianę wykonaną z niejednorodnego materiału. Analiza dotyczy powszechnie stosowanych ścian wykonanych z: cegieł pełnych oraz klinkierowych zawierających 18 lub 30 pionowych otworów. Zaprezentowano i omówiono wpływ wewnętrznej geometrii i objętościowej gęstości cegieł na rozkład pola. Zbadano również wpływ elektrycznej przewodności materiału cegieł. Prezentowane wyniki i dyskusja dotyczą rozkładu pola wokół materiału złożonego z nieidealnych, absorbujących dielektryków. (*Niejednorodność i tłumienie pola elektromagnetycznego wielkiej częstotliwości w bliskim obszarze porowatej ściany*).

**Keywords:** electromagnetic wave propagation, finite difference time domain method (FDTD), wireless communication, building materials  
**Słowa kluczowe:** propagacja fali elektromagnetycznej, komunikacja bezprzewodowa, materiały budowlane: cegła.

### Introduction

The contemporary development of wireless communication networks (e.g. Wi-Fi) demands detailed analysis of the phenomena connected with the propagation of electromagnetic (EM) waves inside buildings. Designing of a reliable Wi-Fi system requires taking into account some modifications and distortions of the electromagnetic field caused by multiple reflections, diffractions, selective dumping and changes of the wave number in different materials. These phenomena are especially important in typical buildings, where the electromagnetic wave propagates between a transmitter and a base station through a number of complex material structures.

The walls can be made of different materials e.g. clay brick, aerated concrete, concrete, wood, glass. Implementation of them depends on wide number of factors and the distribution of EM field usually plays a minor role in that case.

The effects connected with propagation of EM field across construction materials have been the subject of some investigations [1-8]. A lot of models consist of homogeneous slab described by some effective, aggregated values of two electrical parameters i.e.  $\varepsilon=\varepsilon_0 \cdot \varepsilon_r$  - electric permittivity and  $\sigma$  - conductivity [9]. The wall made of concrete with air holes was discussed in some papers. This type of construction (i.e. the cinder blocks) is used in the UK [10]. Recently, the framework constructions in Poland, are made of different types of brick, aerated concrete or a kind of ceramics.

The next question is connected with the right selection of electrical properties. This is particularly questionable when the properties of complex material are homogenized. In that case the authors apply various data to describe electric parameters of materials [3, 5, 11, 13-14]. Some authors assume a proportional relation between permittivity and frequency (e.g.  $\varepsilon_r=3.7 \div 19$ , properly  $f=3 \div 24$  GHz) [13]. Opposite dependencies are examined in some other papers ( $\varepsilon_r=4.62 \div 4.11$ ,  $f=1.7 \div 18$  GHz) [14]. The range of conductivity of a brick material is significantly wide ( $\sigma=0.00278 \div 0.244$  S/m) [11, 14-15].

In this paper the distribution of electromagnetic field inside and in the area close to the brick wall is analysed. Two typical kinds of brick were taken into account: with 18 and with 30 holes. The resulting electric properties of the wall were changed according to relative volume as well as

conductivity of clay solid. These factors are analysed and discussed using a periodic infinite model of the wall.

### Description of analysed model

The interactions of electromagnetic field and the concrete slab were presented in the previous studies [18]. The main trouble was the correct choice of material properties of a homogeneous solid. Only some thin wires of the reinforcement bring on some local disturbances. Their properties can be appropriately modelled by implementation of perfect electric conductor (PEC) boundary condition [19].

In this paper two walls made of hollow clay brick were analysed:

- brick with 18 holes ( $C_{18}$ ) (Fig. 1a),
- brick with 30 holes ( $C_{30}$ ) (Fig. 1b).

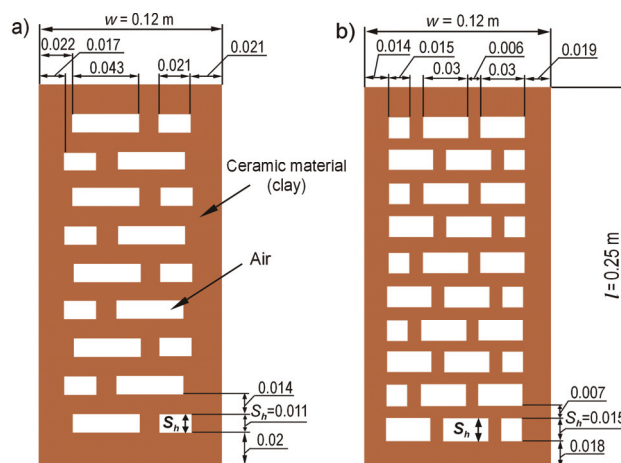


Fig.1. Two kinds of the analysed bricks (2D view, perpendicular to the plane XZ): a) the brick with 18 holes ( $C_{18}$ ) and b) the brick with 30 holes ( $C_{30}$ )

To compare the field phenomena, the additional solid wall (i.e. made of bricks without holes) was taken into account.

The structure of the brick remains complex and heterogeneous. Due to different analysed cases of brick it was assumed of changeable width of air holes ( $s_n$ ) but the outside height ( $h$ ), width ( $w$ ) and length ( $l$ ) were the same, i.e.  $0.065 \times 0.12 \times 0.25$  m (Figs. 1, 2).

The presented problem is appropriate to a model with an electrically porous material. The wave propagates through a multi-layered and split structure of the air and a non-ideal, dissipative clay. The resultant electrical image of the  $C_{18}$  and  $C_{30}$  bricks arose due to the electromagnetic field theory are presented in Fig. 2. The lengths of the subsequent parts are related to wavelength in the air and clay, respectively. The sizes of the air holes ( $s_h$ ) and parts made of the clay are almost the same. The dimensions of typical parts are approximately comparable to the wavelength ( $\lambda$ ). For a lossless dielectrics the length of the EM wave is presented by equation:

$$(1) \quad \lambda = \frac{c}{f \sqrt{\epsilon_r \mu_r}}$$

where:  $f$  is the frequency of wave,  $c$  – the speed of the EM wave in the vacuum.

For all analysed cases the constant value of the permittivity was assumed  $\epsilon_r=4.44$  [11, 14]. The conductivity was changed in the range  $\sigma=0\div0.2$  S/m. In the analysed cases the wavelength in the air was  $\lambda_a=0.125$  m and inside the brick it was changed according to  $\epsilon_r$  and  $\sigma$ . Its approximate value  $\lambda_b$  was equal 0.0593 m.

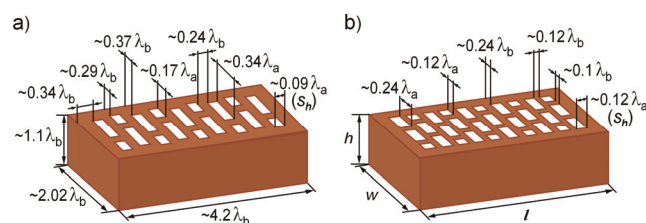


Fig.2. Electrical sizes of two kinds of analysed bricks (3D view): a)  $C_{18}$  brick and b)  $C_{30}$  brick

It is obvious, that some parts of the brick can take on untypical size after the firing process (i.e. drying and hardening). Therefore the influence of a different relative volume of the clay on the wave propagation was analysed. This factor was modified by changing the size of air holes ( $s_h$ ) (Table 1). The usual average size of air holes ( $s_h$ ) in  $C_{18}$  brick is 0.011 m (Fig. 1a) and in  $C_{30}$  – 0.015 m (Fig. 1b).

Table 1. Percentage of the total brick volume inside the two types of brick with different size of the holes

Size of holes ( $s_h$ ) inside the bricks, along X-axis (Fig. 2)		Relative volume of the clay in the brick [%]	
Geometric size [m]	Electric size [m]	Type $C_{18}$	Type $C_{30}$
0.005	0.040 $\lambda_a$	90.40	87.50
0.007	0.056 $\lambda_a$	86.56	82.50
0.009	0.072 $\lambda_a$	82.72	77.50
0.011	0.088 $\lambda_a$	78.88	72.50
0.013	0.104 $\lambda_a$	75.04	67.50
0.015	0.120 $\lambda_a$	71.20	62.50
0.017	0.136 $\lambda_a$	67.36	57.50
0.019	0.152 $\lambda_a$	63.52	52.50

In this analysis the particular attention is paid to the wave behind the infinitely stretched wall (Fig. 3). In the presented case the length of the wall is larger than the size of a single brick and the length of EM wave. The field phenomena in X direction is approximated using the

periodic boundary conditions. The length of the wall was reduced to only three bricks and the Bloch periodic BC conditions were assumed on the edges perpendicular to X axis. The fields on one side of the computational cell are copied from the other side of the computational cell, multiplied by the complex phase  $\exp(j \mathbf{k} \cdot \mathbf{x})$ , where  $\mathbf{k}$  is the Bloch wave vector propagation,  $x$  – the length of computational area in the X direction [17].

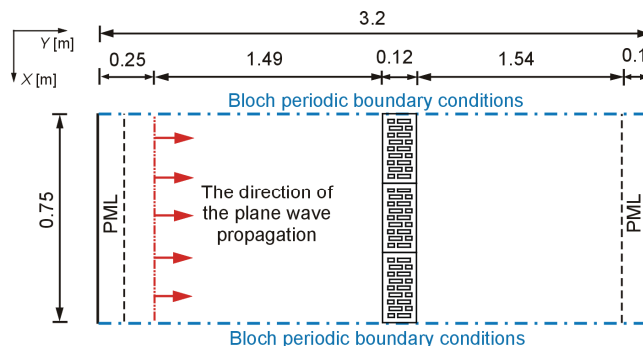


Fig.3. Geometry and physical constraints of analysed model (the  $C_{18}$  bricks)

A plane wave with a sinusoidal carrier of frequency  $f=2.4$  GHz (typical to Wi-Fi) illuminated the analysed structure. The EM field is excited in a region far away of the wall. The absorption of the incident and reflected waves are obtained using PML boundary conditions [12]. They are inscribed in the outer regions perpendicular to the direction of propagation (Fig. 3).

### Numerical model

To determine the distribution of the electromagnetic field the finite difference time domain method (FDTD) was used [12]. This method is useful in the numerical analysis of some broadband and high frequency time dependent electromagnetic fields. One of the advantage is its simple implementation and easy handling of complex geometries using structures of usually regular mesh.

The FDTD method is based on the direct numerical integration of the Maxwell curl equations in time and space [8, 12, 16]. The examined area is divided into elementary cubic Yee cells. The stability of the time marching explicit scheme requires satisfying the Courant-Friedrichs-Lewy (CFL) condition [12, 16]. In 2D case it defines the dependence between the minimum value of the integration step in the time domain  $\Delta t$  and the maximum size of the Yee cell

$$(2) \quad \Delta t \leq \frac{1}{c \sqrt{\frac{1}{(\Delta x)^2} + \frac{1}{(\Delta y)^2}}}$$

where  $\Delta x$ ,  $\Delta y$  are sizes of a dimensions of a cubic element in X and Y directions respectively. The whole area was composed of Yee cells measuring 0.0016667 m on each direction. The total number of cells for each models were to 864 000.

The evaluation of the electromagnetic field distribution was carried out with libraries delivered within the Meep package [17].

### Simulation results

Figure 4 shows the distribution of  $E_z$  component behind and in front of the analysed wall. The results of calculation are shown in the XY plane at the same time, as soon as the steady state of the EM field distribution had been achieved.

The first the maximum value of EM field is reduced behind the wall because the clay in the brick is assumed as a dissipative material ( $\sigma \neq 0$ ). The second reason of the field reduction is the partial reflection of the wave on the borders between two dielectrics.

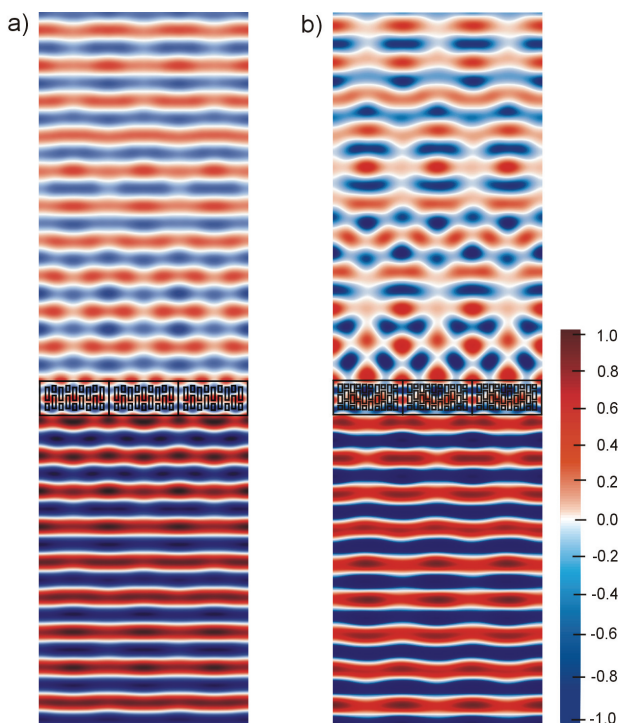


Fig.4. A snapshot of the 2D distribution of relative value of  $E_z$  component in area of the wall made of typical bricks: a)  $C_{18}$  and b)  $C_{30}$

The geometry of the analysed configurations is fairly simple, repeatable, fitting within the Cartesian coordinate system. However, the assessment of the occurrence within the analysed configurations may be conducted only by means of numerical methods. Analytical solution of the presented problem is not possible when taking into account the distribution of material within the brick. For the same reason, the acquired calculation results are not entirely predictable and uniformly interpreted. The EM waves propagation in the area of the brick is of complex character. The porousness of the brick in the electromagnetic sense results in the appearance of multiple reflections on the line air-brick. For this reason, as seen in fig. 4, the amount of holes in the brick changes the image of the field in the area close behind the wall. In Fig. 4 the difference in relative volume of the clay inside the  $C_{18}$  and  $C_{30}$  bricks was 16.38%.

The local change of the wave velocity during the passing over the different areas of brick cause to appear the instantaneous images of the field which indicate on wave interference formation. Described effect is particularly visible during the evaluation of phenomenon which occur behind the wall made of  $C_{30}$  bricks. In comparison, the value of the fields behind the two kinds of wall in part vindicate this phenomena. The distribution of the field which there is behind the wall ( $C_{30}$  bricks) contains higher values of both maximum and minimum.

As indicated before, the assessment of the observed electromagnetic occurrences, due to the structure of the configuration, is not obvious and uniform. The previously analysed differences in field value in both cases may be explained by analysing the amount of loss dielectric. The decline in relative amount of the dielectric in the area of  $C_{30}$

brick causes lesser blocking of the wave passing through the wall. This causes the value of the field behind the  $C_{30}$  wall to be higher that with the  $C_{18}$  brick. In accordance with Fig. 5-6, the increase in field value with the  $C_{30}$  brick, is especially visible with the increase of the relative size of air holes (i.e. lowering the relative part of the lossy dielectric). In front of the analysed wall the situation is reversed. It is visible the increase of maximum values of  $E_z$  component in  $C_{18}$  model (Fig. 4a).

Figures 5 and 6 show the relative maximum values of the  $E_z$  component and their dependencies on the size of holes ( $s_h$ ). The subsequent curves are made for different values of the electric conductivity of the brick. Since the value of  $\sigma$  depends on the quality of material and humidity of the wall, these figures give information about different conditions. When the dissipation factor  $\sigma$  increases the resultant value of the field decreases.

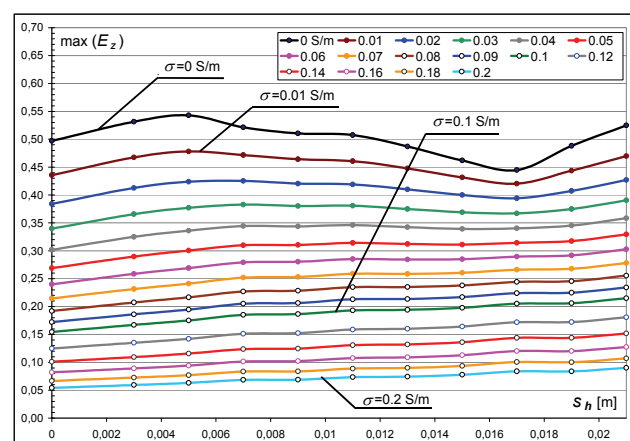


Fig.5. The relative maximum values of  $E_z$  component behind the wall made of  $C_{18}$  bricks as a function of the width of air holes

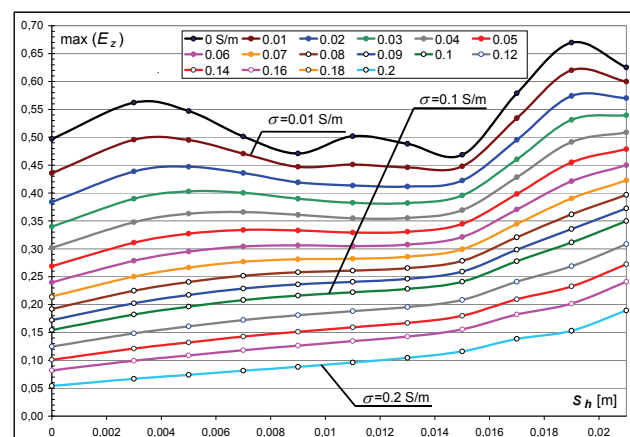


Fig.6. The relative maximum values of  $E_z$  component behind the wall made of  $C_{30}$  bricks as a function of the width of air holes

In case  $C_{18}$  brick (Fig. 5) the characteristics, which were obtained for different  $\sigma$  and  $s_h$ , show that when the size of air holes increases, the maximum values of  $E_z$  component also increase. But for  $\sigma=0 \div 0.04$  S/m are visible dip of this value especially for  $s_h=0.013 \div 0.014$  m. In Fig. 6, where the case of  $C_{30}$  brick was presented, the characteristics are less regular than in the previous model ( $C_{18}$ ). This picture presents two visible increases of maximum values of  $E_z$  component ( $s_h=0.003 \div 0.005$  m and  $s_h=0.017 \div 0.019$  m), especially when the conductivity is in the range of  $\sigma=0 \div 0.04$  S/m. In these cases the size of the air holes is not use in this kinds of brick in building technology.



An increase in the relative usage of a lossless dielectric at area of the brick causes the value of the field to be higher. The observed changes are especially visible in cases which have a low lossless material like a clay. Increase in the material's lossness causes that the principal role in phenomena process has the damping of the wave at crossing over dielectric. The change of air holes size cause barely twice higher the maximum values of field in case  $C_{18}$  bricks but in  $C_{30}$  bricks values are four times higher.

During the analysis of a wall which wave attenuation is low (e.g.  $\sigma < 0.01$  S/m) or equal zero, the major role has interference effects. This reason explains non-monotonic process of characteristics and also visible minimum at the range of size of air holes ( $s_p$ ). It is important that this process is observed only for characteristics with almost lossless material. The indicated effect can be a result of waves passing over porous medium. In this kind of medium more important are effects of partial diffraction of wave and local change its propagation of wave velocity.

## Conclusions

Electromagnetic wave propagation across porous walls is examined as a complex process. In case the macroscopic analysis of building areas the homogenisation of material properties of components is essential due to it limiting the computational power of a PC computer. One of the important restriction, which forces this approach, is difficulty mapping the real complex walls.

The complex character of observed phenomena is partially validated. The aim of realized tests was defined by the influence of the size of air holes on the value of field behind the wall.

The analysis of the obtained results has indicated that some reflections, diffractions and absorption in the complex wall change the final distribution of EM field in the front and behind the wall. If percentage of the brick's volume decreases, the distribution of EM field will become more irregular and then might appear the local increase or decreases of the values of EM field at near distance from the wall. Presented results are caused by multiple reflections especially from edges of the holes inside brick, diffractions and absorption in the complex wall, which change the final distribution of EM field both in the front of and behind the wall.

Further research will focus on the influence of the irregularities of the holes and different construction materials used for the walls which are made of the brick.

## REFERENCES

- [1] Richalot E., Bonilla M., Wong M., Fouad-Hanna V., Baudrand H., Wiart J., Electromagnetic propagation into reinforced-concrete walls, *IEEE Transactions on Microwave Theory and Techniques*, 48 (2000), No. 5, 357-366
- [2] Cuinas I., Sanchez M.G., Permittivity and conductivity measurements of building materials at 5.8 GHz and 41.5 GHz, *Wireless Personal Communications*, 20 (2002), 93-100
- [3] Stavrou S., Saunders S.R., Review of constitutive parameters of building material, *IEEE Transactions on Antennas and Propagation*, Vol. 1 (2003), 211-215
- [4] Antonini G., Orlandi A., D'elia S., Shielding effects of reinforced concrete structures to electromagnetic fields due to GSM and UMTS systems, *IEEE Transactions on Magnetic*, 39 (2003), No. 3, 1582-1585
- [5] Dalke R.A., Holloway Ch.L., McKenna P., Johannson M., Ali A.S., Effects of reinforced concrete structures on RF communications, *IEEE Transactions on Electromagnetic Compatibility*, 42 (2000), No. 4, 486-496
- [6] Liu Ping, Chen Gui, Long Yun-liang, Effects of reinforced concrete walls on transmission of EM wave in WLAN, *Proceedings of the ICMMT 2008, International Conference on Microwave and Millimeter Wave Technology*, Vol. 2 (2008), 519-522
- [7] Choroszucho A., Pieńkowski C., Jordan A., Electromagnetic wave propagation into building constructions, *Przegląd Elektrotechniczny*, 84 (2008), nr 11, 44-49
- [8] Weiping Q., Shenggao D., Yerong Z., FDTD Calculation of the Effects of Reinforced Concrete Wall on Short Path Propagation of UWB Pulse, *IEEE Microwave Conference Proceedings, APMC 2005. Asia-Pacific Conference Proceedings (2005)*
- [9] Peña D., Feick R., Hristov H.D., Grote W., Measurement and modeling of propagation losses in brick and concrete walls for the 900 MHz band, *IEEE Transactions on Antennas and Propagation*, 51 (2003), No. 1, 31-39
- [10] Yang M., Stavrou S., Rigorous coupled-wave analysis of radio wave propagation through periodic building structures, *IEEE Antennas and Wireless Propagation Letters*, Vol. 3 (2004), 204-207
- [11] Tan S.Y., Tan Y., Tan H.S., Multipath delay measurements and modeling for interfloor wireless communications, *IEEE Transactions on Vehicular Technology*, 49 (2000), No. 4, 1334-1341
- [12] Taflove A., Hagness S.C., Computational electrodynamics, The Finite-Difference Time-Domain Method. Boston, Artech House, (2005)
- [13] Shah M.A., Hasted J.B., Moore L., Microwave absorption by water in building materials: aerated concrete, *British Journal of Applied Physics*, Vol. 16 (1965), No. 11, 1747-1754
- [14] Landron O., Feuerstein M.J., Rappaport T.S., A comparison of theoretical and empirical reflection coefficients for typical exterior wall surfaces in a mobile radio environment, *IEEE Transactions on Antennas and Propagation*, Vol. 44 (1996), No. 3, 341-351
- [15] Pinhasi Y., Yahalom A., Petnev S., Propagation of ultra wide-band signals in lossy dispersive media, *IEEE International Conference on Microwaves, Communications, Antennas and Electronic Systems, COMCAS (2008)*, 1-10
- [16] Luebbers R.J., Kunz K.S., The finite difference time domain method for electromagnetism, CRS Press (1993)
- [17] Oskooi A.F., Roundyb D., Ibanescua M., Bermelc P., Joannopoulousa J.D., Johnson S.G., MEEP: A flexible free-software package for electromagnetic simulations by the FDTD method, *Computer Physics Communications*, Vol. 181 (2010), 687-702
- [18] Choroszucho A., The influence of reinforcing steel meshes inside the concrete wall on electromagnetic field distribution, *Pomiary, Automatyka, Kontrola*, Vol. 56 (2010), No. 2, 104-106
- [19] Choroszucho A., Butryło B., Local attenuation of electromagnetic field generated by wireless communication system inside the building, *Przegląd Elektrotechniczny*, R. 87 (2011), nr 7, 123-126

## Authors:

mgr inż. Agnieszka Choroszucho,  
E-mail: [a.choroszucho@pb.edu.pl](mailto:a.choroszucho@pb.edu.pl),  
dr inż. Bogusław Butryło, E-mail: [b.butrylo@pb.edu.pl](mailto:b.butrylo@pb.edu.pl)  
Politechnika Białostocka, Wydział Elektryczny, Katedra  
Elektrotechniki Teoretycznej i Metrologii, ul. Wiejska 45D, 15-351  
Białystok.